2014

Increasing the Neel temperature of magnetoelectric chromia for voltage-controlled spintronics

M Street
University of Nebraska-Lincoln

W Echtenkamp
University of Nebraska-Lincoln

Takashi Komesu
University of Nebraska-Lincoln, tkomesu2@unl.edu

Shi Cao
University of Nebraska-Lincoln, caoshi86@gmail.com

Peter A. Dowben
University of Nebraska-Lincoln, pdowben@unl.edu

See next page for additional authors

Increasing the Néel temperature of magnetoelectric chromia for voltage-controlled spintronics

M. Street, W. Echtenkamp, Takashi Komesu, Shi Cao, P. A. Dowben, and Ch. Binek
Department of Physics and Astronomy, Nebraska Center for Materials and Nanoscience, Theodore Jorgensen Hall, 855 North 16th Street, University of Nebraska, P.O. Box 880299, Lincoln, Nebraska 68588-0299, USA

(Received 18 March 2014; accepted 20 May 2014; published online 2 June 2014)

Boron doped chromia (Cr_2O_3) thin films with substitutional doping levels between zero and 3% are grown using pulsed laser deposition in borane background gases. Magnetometry reveals a tunable increase in the Néel temperature of the (0001) textured $Cr_2B_xO_{3-x}$ thin films at a rate of about 10% with 1% oxygen site substitution preserving a net boundary magnetization. Spin resolved inverse photoemission measured after magnetoelectric annealing in subsequently reversed electric fields evidences voltage-controlled reversal of boundary magnetization and thus magnetoelectricity of $Cr_2B_xO_{3-x}$. Conservation of magnetoelectricity far above room temperature makes ultra-low power voltage-controlled spintronic devices feasible. © *2014 AIP Publishing LLC*.
[http://dx.doi.org/10.1063/1.4880938]

Today's emerging spintronic devices aim at the unabated continuation of an exponentially growing performance-cost ratio.[1] A key property of spintronic devices is the inherent non-volatility of remnant magnetization which allows for retention of the state variable in spintronic nanostructures without energy consuming refreshing cycles. In order to implement writing of magnetic bits at ultra-low power, the search for voltage-controlled switching of magnetic state variables, which does not rely on electric currents, has intensified.[2–4] In this regard, voltage-controlled exchange bias is particularly promising if reliable at room temperature and achievable with low coercive voltages. Exchange bias occurs because of exchange interaction at the interface of adjacent ferromagnetic and antiferromagnetic thin films creating unidirectional anisotropy in the ferromagnetic layer. It shifts the ferromagnetic hysteresis loop along the magnetic field axis by an amount known as the exchange bias-field.

There are at least two coexisting approaches utilizing exchange bias for voltage-control of magnetization. One strategy relies on the use of multiferroic antiferromagnets, and most notably the multiferroic $BiFeO_3$, to pin the adjacent ferromagnetic film. $BiFeO_3$ films strained through substrate lattice mismatch, have been engineered to enable electric switching of the ferromagnetic hysteresis in zero applied magnetic field.[5] This remarkable breakthrough is still limited to temperatures far below room temperature.[6] An alternative approach takes advantage of magnetoelectric antiferromagnets such as the archetypical Cr_2O_3[7–11] or Fe_2TeO_6.[12] In contrast to multiferroics, magnetoelectric antiferromagnets possess no spontaneous ferroelectric polarization but, nevertheless, allow for isothermal voltage-control of the antiferromagnetic interface magnetization. Cr_2O_3-based exchange bias systems are perhaps the most promising pathway to voltage-control of exchange bias at room temperature when allowing for the presence of a small symmetry breaking static magnetic field during the electric switching of the antiferromagnetic order parameter.[8,9] All exchange bias systems have in common that antiferromagnetic interface magnetization couples via exchange with the adjacent ferromagnet giving rise to the exchange bias effect.[13,14] In magnetoelectric antiferromagnets, however, this interface magnetization (boundary magnetization) has a unique origin and distinctive properties with important consequences for voltage-control of exchange bias.[15,16] Roughness insensitive boundary magnetization emerges at surfaces or interfaces of a single domain magnetoelectric antiferromagnet.[17] This phenomenon originates from the symmetry conditions associated with magnetoelectricity and gives rise to an intimate coupling between the boundary magnetization and the antiferromagnetic order parameter.[14] In chromia, the antiferromagnetic order parameter can be switched by an electric field in the presence of a simultaneously applied magnetic field.[18] The reversal of the antiferromagnetic order parameter is accompanied by reversal of the boundary magnetization which causes the exchange bias field of the ferromagnetic film to switch.[9]

Bulk chromia has a Néel temperature of about 307 K.[19] Above this ordering temperature, time inversion symmetry is reestablished and the linear magnetoelectric effect is ruled out by symmetry constraints. In order to tune the magnetoelectric properties of chromia towards the requirements of room temperature spintronic applications, its Néel temperature, T_N, in thin films needs to be increased by at least 50 K relative to $T_N = 307$ K of bulk chromia.

There are two prominent approaches to engineer an increase in the critical temperature of chromia. One is the use of strain to increase the intralayer antiferromagnetic exchange between Cr^{3+} ions by increasing the orbital overlap.[20,21] This concept is theoretically well established. However, experimental results showing strain-induced effects on the antiferromagnetic ordering are still controversial. Recently, a dramatic increase in the magnetoelectric susceptibility of chromia nanoparticles has been reported.[22] The authors of Ref. 22 interpret the increase of the magnetoelectric response in terms of a strain-induced effect. We find it far more likely that the reported observation reveals an increase in the effective magnetoelectric susceptibility as a result of the increase in the number of surface spins

contributing to boundary magnetization in nanosized chromia particles relative to the bulk in a nanoparticle.

Increasing the Néel temperature in chromia thin films via strain through lattice mismatch with the substrate requires epitaxy to avoid relaxation of stresses from grain boundaries.[23] However, epitaxial growth of films is not favorable for device applications. In addition, generally voltage-control cannot currently be scaled down to a few nm thickness in chromia thin films due to dielectric deficiencies accompanying the various growth methodologies.[27] In this Letter, we demonstrate a sizable and tunable T_N increase of chromia films via substitutional anion doping and demonstrate the possibility to voltage-control the boundary magnetization in doped films.

First principles investigations have shown that boron substituting oxygen can increase the exchange energies between Cr spins and thus increase the antiferromagnetic ordering temperature.[24] Boron substituting oxygen, due to the favorable hybridization geometry, can strengthen ferromagnetic coupling between those Cr sites with the same spin orientation. This ferromagnetic coupling reinforces the antiferromagnetic order and enhances the exchange energies, thus increasing the antiferromagnetic ordering temperature. The calculations show each B atom enhances the exchange energy on its four Cr neighbors by a factor of 2–3 and that substitutional boron doping of Cr_2O_3 can increase T_N by roughly 10% per 1% O site substitution with B. We follow this theoretical prediction fabricating (0001) textured and B-doped chromia thin films through pulsed laser deposition (PLD) methodology. Deposition takes place in a decaborane ($B_{10}H_{14}$) vapor background of various partial pressures between $\sim 7.5 \times 10^{-8}$ and 1.0×10^{-6} millibars resulting in doping levels between $x \approx 0$ and approximately 3%, as determined from core level photoemission. Decaborane is known for its use in doping of many semiconductors.[25]

Here, pulsed laser deposition of Cr_2O_3 from a chromia target in the presence of $B_{10}H_{14}$ background atmosphere leads to substitution of O^{2-} ions by boron. We used a KrF excimer laser with pulse energies of 200 mJ and pulse width of 20 ns at a repetition rate of 10 Hz to create a plume from a chromia target allowing to deposit (0001) textured chromia thin films on cleaned sapphire (0001) substrates. The substrates are kept at 700 °C during deposition and are located ~8.5 cm from the target.

Figs. 1(a) and 1(b) show the structural characterization of our films through wide angle $\theta - 2\theta$ x-ray diffraction patterns of undoped (Fig. 1(a)) and approximately 3% B-doped (Fig. 1(b)) chromia (0001)-textured thin films in accordance with narrow (0006) and (00012) Bragg-peaks. Note that the (0006) and (00012) peaks of the dilute sample are slightly shifted by about 0.4° to lower angles relative to the undoped sample. This finding is in good agreement with fully relaxed first principle calculations which confirm a small increase in the c-axis on B-doping.[26] The insets show the respective small angle x-ray diffraction images allowing to determine the film thicknesses of the undoped and B-doped films to 26.3 nm and 35.5 nm with roughness of 0.22 nm and 0.26 nm, respectively.

Fig. 2 shows the temperature dependence of the remnant magnetic moment, m, of all investigated samples reflecting

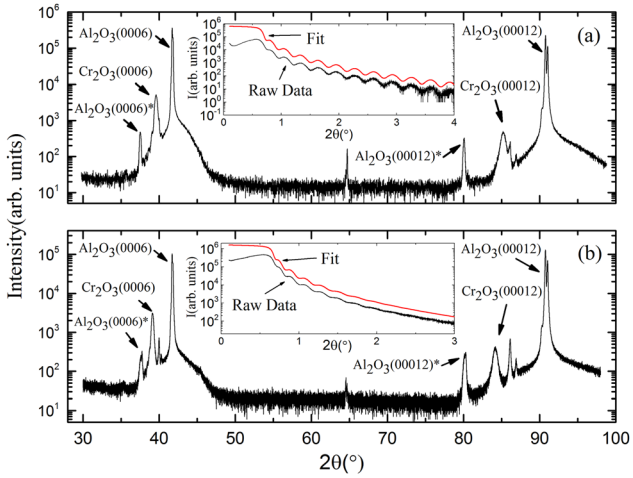

FIG. 1. Wide and small angle x-ray diffraction of pure (a) and B-doped (b) chromia thin films. Narrow (0006) and (00012) K_α peaks indicate (0001) textured chromia. (*) indicates K_β peaks. Inset of (a) shows small angle x-ray diffraction raw data and best fit (shifted for clarity relative to raw data) determining a film thickness of 26.3 nm and roughness of 0.22 nm. Panel (b) and inset show the corresponding data for 3% B-doped chromia thin film. Fit of x-ray small angle diffraction data reveals a film thickness of 35.5 nm with roughness of 0.26 nm.

the boundary magnetization of pure and B-doped chromia films. The m vs. T data have been measured with a superconducting interference device (SQUID) on zero field heating after field-cooling the films in a magnetic field of 7 T applied normal to the films. True zero-field conditions have been maintained on heating through quenching of the superconducting coils, thus eliminating residual trapped magnetic flux. It has been previously shown that, in the case of thin films, magnetic field-cooling suffices to select a preferential orientation of the boundary magnetization in the direction of the applied field.[27] Note that a net boundary magnetization can be measured by integral magnetometry due to the nonequivalence between the chromia/vacuum boundary and the chromia/sapphire boundary. The preferential selection of

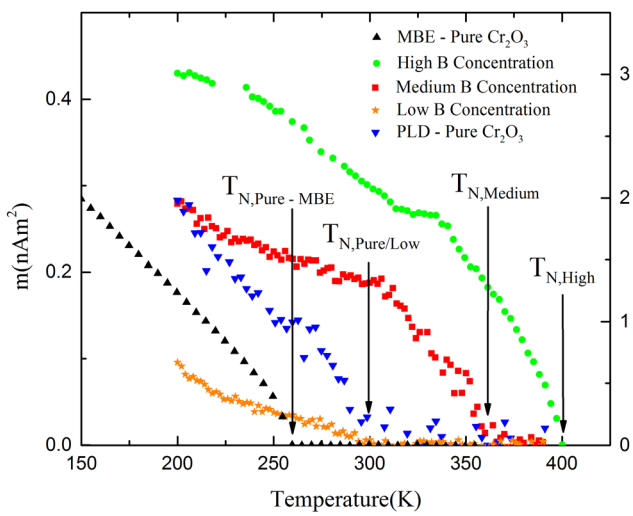

FIG. 2. Magnetic moment, m, versus temperature measured on heating in zero applied field for PLD grown films of pure chromia (down triangles) and B concentrations from <1% (stars) to ~2% (squares) to ~3% (circles). Samples were field-cooled in the presence of 7 T normal to the film from 400 K to 200 K. Up triangles show reference zero-field heating data for a pure chromia film of 100 nm thickness grown by molecular beam epitaxy.

boundary magnetization is accompanied and stabilized by preferential selection of one of the two degenerate 180° antiferromagnetic single domain states. Because the remnant boundary magnetization is intimately coupled with the antiferromagnetic order parameter, the temperature T^* defined by $m(T > T^*) = 0$ unambiguously determines the Néel temperature, T_N, of the film. In accordance with the theoretical prediction,[23] we find an increase in T_N with increasing B-concentration from $T_N(x = 0) \approx 307$ K to $T_N(x \approx 0.03) \approx 400$ K. For reference purposes, we show our data measured from a sample of 28 nm thickness grown by molecular beam epitaxy.[28] Note that in thin films $T_N(x = 0) < 307$ K is commonly observed (see up triangle Fig. 2). Here, finite size effects and defects such as potential oxygen vacancies can reduce the Néel temperature substantially to below the bulk value.[29] This fact highlights the challenge and achievement associated with increasing the Néel temperature in thin films to values as high as $T_N(x \approx 0.03) \approx 400$ K via B-doping.

The various undoped and B-doped PLD grown chromia thin films have been investigated by spin-polarized inverse photoemission experiments. The significance of the inverse photoemission experiments lies in the fact that their unmatched surface sensitivity allows us to determine whether the B-doped films possess boundary magnetization and whether this boundary magnetization can be switched via voltage-control, a necessary prerequisite for their use in potential room temperature spintronic applications.

Our experiments utilize a transversely polarized spin electron gun based upon the Ciccacci design.[30] The spin electron gun was designed in a compact form on a separate chamber equipped with an iodine based Geiger-Mueller isochromat photon detector with a SrF_2 window, with base pressure of 3.0×10^{-10} millibars or better. As is typical of such instruments, the electron gun has 28% spin polarization, and the data have been corrected for this incident gun polarization. The direction of electron polarization is in the plane of the sample. The energy resolution was in the vicinity of 400 meV. The magnetoelectric cooling was accomplished in an axial magnetic field of >40 mT and a voltage of 1400 V applied across the film thickness. The Fermi level was established from tantalum and gold foils in electrical contact with the sample. Typically, many experiments are summed, to improve the signal-to-noise ratio in the spin-polarized inverse photoemission spectra. The 3% doped samples provide very significant spin polarization asymmetries at room temperature, compared to undoped chromia.

Fig. 3 shows the spin polarized inverse photoemission of B-doped chromia thin films with doping concentration <1% (Fig. 3(a)) and a B-doped chromia of about 3% (Fig. 3(b)). Spin up and spin down channels are represented by up and down triangles. The lines represent the respective average inverse photoemission signal. The spectrum of low B-doped samples (Fig. 3(a)) measured at $T = 295$ K shows no appreciable spin polarization, similar to undoped chromia. However, Fig. 3(b) depicts the spin resolved inverse photoemission spectra of the 3% doped sample with significant spin polarization at room temperature. Electric field switching was demonstrated together with control experiments in non-spin-mode over several samples. A key result is that the boundary magnetization is seen to reverse when the electric field is reversed

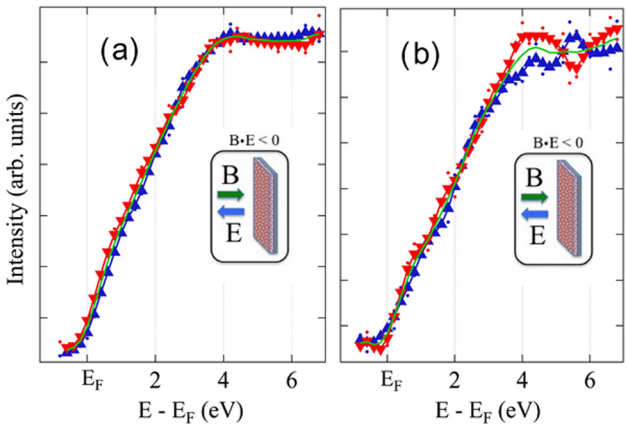

FIG. 3. Spin-polarized inverse photoemission spectra taken at 295 K after field cooling with B•E < 0. Data are shown for Boron concentrations less than 1% (a) and approximately 3% (b), as determined from XPS core level intensities. Spin majority–spin up state, and spin minority–spin down state, components are indicated by upward triangles and downward triangles, respectively, as a smoothed spectra result. The green lines are spin integrated spectra.

during field cooling to $T = 295$ K. This confirms a magnetoelectric origin to this boundary magnetization together with the fact that sizable boundary magnetization is present at $T = 295$ K. The spectra of the doped samples are in contrast to the spectra of the undoped samples where the antiferromagnetic order parameter and the boundary magnetization are too low at $T = 295$ K to allow resolving voltage-controlled switching via inverse photoemission. The photoemission data are thus consistent with the data from SQUID magnetometry shown in Fig. 2 and moreover confirm that B-doped samples with increased Néel temperature have voltage-controllable boundary magnetization. The less the boron content, the less pronounced is the in-plane spin asymmetry at room temperature. This can be interpreted as an increase of the Néel temperature with increasing B-concentration in accordance with the results from magnetometry.

In conclusion, we have shown that B-doping of the magnetoelectric antiferromagnet chromia is an efficient way to increase the Néel temperature. Our experimental findings obtained by SQUID magnetometry and spin polarized inverse photoemission spectroscopy are in good agreement with first principle investigations predicting an increase of the Néel temperature by approximately 10% per 1% substitution of oxygen by boron. Our magnetometry data reveal an increase of the critical temperature of chromia from its bulk value of 307 K to 400 K by approximately 3% boron doping. The findings are of utmost significance for the use of chromia and potentially other magnetoelectric antiferromagnets in ultra-low power, voltage-controlled spintronic applications. Several challenges remain to be addressed before the vision of spintronic applications can be realized. Boron has an exceptionally small atomic radius and hence is prone to diffusion. We have indications that our samples suffer from B-diffusion after repeated heat treatment. In addition, it is still an open question whether B only occupies oxygen positions in the lattice. Our core level shifts observed from x-ray spectroscopy seem to indicate that this is indeed the case in the bulk, but imply that at the surface chromium positions can also be occupied by boron. Our investigations create an

antiferromagnetic material in thin film geometry suitable for practical room temperature voltage-controlled spintronics and thus pave the way for future spintronic device applications.

This project was supported by the Semiconductor Research Corporation through the Center for Nanoferroic Devices, an SRC-NRI Center under Task ID 2398.001, by C-SPIN, part of STARnet, a Semiconductor Research Corporation program sponsored by MARCO and DARPA (No. SRC 2381.001) and by the NSF through Nebraska MRSEC DMR-0820521 and DMR 0747704.

[1]G. E. Moore, Electronics **38**, 114 (1965).
[2]F. Zavaliche, T. Zhao, H. Zheng, F. Straub, M. P. Cruz, P. L. Yang, D. Hao, and R. Ramesh, Nano Lett. **7**, 1586 (2007).
[3]E. Y. Tsymbal and H. Kohlstedt, Science **313**, 181 (2006).
[4]T. Maruyama, Y. Shiota, T. Nozaki, K. Ohta, N. Toda, M. Mizuguchi, A. A. Tulapurkar, T. Shinjo, M. Shiraishi, S. Mizukami, Y. Ando, and Y. Suzuki, Nat. Nanotechnol. **4**, 158 (2009).
[5]S. M. Wu, S. A. Cybart, D. Yi, J. M. Parker, R. Ramesh, and R. C. Dynes, Phys. Rev. Lett. **110**, 067202 (2013).
[6]Ch. Binek, Physics **6**, 13 (2013).
[7]M. Fiebig, J. Phys. D: Appl. Phys. **38**, R123 (2005).
[8]P. Borisov, A. Hochstrat, X. Chen, W. Kleemann, and Ch. Binek, Phys. Rev. Lett. **94**, 117203 (2005).
[9]X. Chen, A. Hochstrat, P. Borisov, and W. Kleemann, Appl. Phys. Lett. **89**, 202508 (2006).
[10]X. He, Y. Wang, N. Wu, A. N. Caruso, E. Vescovo, K. D. Belashchenko, P. A. Dowben, and Ch. Binek, Nature Mater. **9**, 579–585 (2010).
[11]W. Echtenkamp and Ch. Binek, Phys. Rev. Lett. **111**, 187204 (2013).
[12]JL. Wang, J. A. Colón Santana, N. Wu, C. Karunakaran, J. Wang, P. A. Dowben, and Ch. Binek, J. Phys.: Condens. Matter **26**, 055012 (2014).
[13]J. Nogués and I. K. Schuller, J. Magn. Magn. Mater. **192**, 203 (1999).
[14]Ch. Binek, *Ising-Type Antiferromagnets: Model Systems in Statistical Physics and in the Magnetism of Exchange Bias*, Springer Tracts in Modern Physics, Vol. 196 (Springer, Berlin, 2003).
[15]K. D. Belashchenko, Phys. Rev. Lett. **105**, 147204 (2010).
[16]A. F. Andreev, JETP Lett. **63**, 758 (1996) [Pis'ma Zh. Éksp. Teor. Fiz. **63**, 724 (1996)].
[17]N. Wu, X. He, A. L. Wysocki, U. Lanke, T. Komesu, K. D. Belashchenko, Ch. Binek, and P. A. Dowben, Phys. Rev. Lett. **106**, 087202 (2011).
[18]T. J. Martin and J. C. Anderson, IEEE Trans. Magn. **2**, 446 (1966).
[19]T. H. O'Dell, *The Electrodynamics of Magneto-Electric Media* (North-Holland, 1970).
[20]K. Belashchenko, private communication (2014).
[21]Y. Kota, H. Imamura, and M. Sasaki, Appl. Phys. Express **6**, 113007 (2013).
[22]D. Halley, N. Najjari, H. Majjad, L. Joly, P. Ohresser, F. Scheurer, C. Ulhaq-Bouillet, S. Berciaud, B. Doudin, and Y. Henry, Nat. Commun. **5**, 1 (2014).
[23]F. Spaepen, Acta mater. **48**, 31 (2000).
[24]S. Mu, A. L. Wysocki, and K. D. Belashchenko, Phys. Rev. B **87**, 054435 (2013).
[25]J. T. Spencer, P. A. Dowben, and Y.-G. Kim, "Deposition of Boron–Containing Films From Decaborane", U.S. patent 4,957,773 (18 September 1990).
[26]S. Mu and K. Belashchenko, private communication (2014).
[27]L. Fallarino, A. Berger, and Ch. Binek, Appl. Phys. Lett. **104**, 022403 (2014).
[28]S. Sahoo and Ch. Binek, Philos. Mag. Lett. **87**, 259 (2007).
[29]X. He, W. Echtenkamp, and Ch. Binek, Ferroelectrics **426**, 81 (2012).
[30]T. Komesu, C. Waldfried, H.-K. Jeong, D. P. Pappas, T. Rammer, M. E. Johnston, T. J. Gay, and P. A. Dowben, Proc. SPIE **3945**, 6–16 (2000).